DOI: 10.1002/adma.200800632

Fluorescent Gold Nanoparticle Superlattices**

By *Naoki Nishida, Edakkattuparambil S. Shibu, Hiroshi Yao, Tsugao Oonishi, Keisaku Kimura,** and *Thalappil Pradeep**

Dedicated to Professor C. N. R. Rao on the occasion of his 75th Birthday.

Metal nanoparticles have a variety of interesting spectroscopic, electronic, and chemical properties that arise from their small sizes and high surface-to-volume ratios.[1–4] Over the last several years, self-assembly of metal nanoparticles into two- or three-dimensional (2D or 3D) ordered arrays has become a topic of increasing interest in the field of nanotechnology.[5–10] The diverse properties of such assemblies have been the driving force for this interest. In earlier papers, we reported the synthesis of single-crystalline 3D superlattices or particle crystals consisting of mercaptosuccinic acid (MSA)-protected gold nanoparticles (Au@MSA). The superlattices form at an air/water interface under highly acidic conditions (<pH 2), and the particles in them are connected through hydrogen bonds between the surface carboxylic acids.[11–16]

Fluorophore-modified gold nanoparticles are important as biological sensors and in optoelectronic devices. The efficiency of emission from electronically excited groups is very sensitive to the location of the fluorophore, which is bound at the outer edge of monolayer-protected metal nanoparticles.[17–19] The latter are well-known quenchers of molecular luminescence. The binding of thiolated fluorophores on gold nanoparticles produced strong, structure-dependent static quenching of the fluorescence intensity.[20–23] Fluorophores can be reversibly bound by electrostatic interactions; an example is the binding of $[Ru(bpy)_3]^{2+}$ to gold nanoparticles with anionic monolayer coatings. This produces strong static luminescence quenching and concurrent weaker collisional or dynamic quenching.[24]

In the work reported in this Communication, we have prepared fluorescent gold nanoparticles and made fluorescent 3D superlattices with them at an air/water interface. Fluorescence spectral images of the superlattices have been examined and compared with those of reference superlattices.

Fluorescein-labeled Au@MSA (denoted Au@MSA/SAMSA where SAMSA is 5-((2-(and-3)-*S*-(acetylmercapto)-succinoyl)amino)fluorescein) was prepared by ligand exchange reaction (see the Experimental Section). Curves a–c in Figure 1 show the absorption spectra of SAMSA, Au@MSA/SAMSA, and Au@MSA, respectively, and curves d–f are the emission spectra of SAMSA, Au@MSA/SAMSA, and Au@MSA, respectively. The left and right ordinates are for absorption and fluorescence spectra, respectively. The spectral profile of Au@MSA is quite similar to that of Au@MSA/SAMSA (surface plasmon band at 540 nm), indicating that no size change of the core occurred. Indeed, the average diameter of Au@MSA/SAMSA (3.43 nm) was similar to that of Au@MSA (3.08 nm), as shown in Figure S1 (Supporting Information).

Although an absorption peak ascribed to the fluorescein moiety (490 nm) could not be observed in Figure 1 (curve b) in the presence of the broad surface plasmon resonance, we could detect distinct emission from the fluorescein moiety at 520 nm (Fig. 1, curve e); the peak maximum was unaffected by binding on the nanoparticle surface (compare with Fig. 1, curve d). The absence of the absorption peak may be due to the very low concentration of the fluorescein molecule on the particle surface.

We performed the exchange reaction of Au@MSA with two different concentrations of SAMSA molecules and calculated the number of SAMSA anchored on the surface of Au@MSA nanoparticles in two different ways. In the first case, we used a very low concentration of SAMSA for the exchange reaction and calculated the number of SAMSA molecules on the basis of the emission intensity. Although an emission quenching of the fluorophores would be expected because of the resonant energy transfer to the metal particles, we tentatively estimated the number of fluorophores on the nanoparticle surface assuming no quenching. From the ratio of the emission intensity of Au@MSA/SAMSA and SAMSA (0.163), SAMSA concentration (1×10^{-6} M), and the solution volume (5 mL), the total number of SAMSA in the probe solution could be estimated as 4.9×10^{14}. On the other hand, the corresponding Au@MSA/SAMSA solution contains 0.2 mg of gold nanoparticles with an average diameter of 3.43 nm, suggesting that the total number of gold nanoparticles is 4.9×10^{14}. Therefore, we

[*] Prof. T. Pradeep, E. S. Shibu
DST Unit on Nanoscience (DST UNS)
Department of Chemistry and
Sophisticated Analytical Instrumentation Facility
Indian Institute of Technology Madras
Chennai 600 036 (India)
E-mail: pradeep@iitm.ac.in
Prof. K. Kimura, Prof. H. Yao, N. Nishida, T. Oonishi
Graduate School of Material Science
University of Hyogo
3-2-1 Koto, Kamigori-cho, Ako-gun
Hyogo 678-1297 (Japan)
E-mail: kimura@sci.u-hyogo.ac.jp

[**] The authors thank the Japan Society for the Promotion of Science and the Department of Science and Technology (DST), Government of India, for funding. The equipment support was provided by the Nanoscience and Nanotechnology initiative of the DST. Supporting Information is available online from Wiley InterScience or from the authors.

ADVANCED MATERIALS

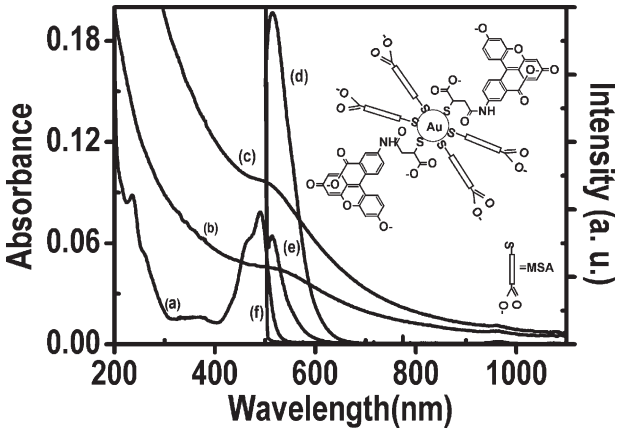

Figure 1. Absorbance spectra of a) SAMSA, b) Au@MSA/SAMSA, and c) Au@MSA, and emission spectra of d) SAMSA, e) Au@MSA/SAMSA, and f) Au@MSA in aqueous solutions. Inset: Scheme of the fluorescent nanoparticle synthesized by exchanging MSA with SAMSA. The left and right ordinate scales correspond to absorption and fluorescence, respectively.

could roughly estimate that one SAMSA molecule is anchored per gold nanoparticle (details are given in calculation 1 in the Experimental section). As this assumes no quenching, it is the minimum value of the surface concentration of SAMSA. In the second case, the concentration of SAMSA used for the exchange reaction was higher and the number of SAMSA molecules on the Au@MSA nanoparticle was calculated using absorption spectroscopy. First, we calculated the number of nanoparticles in the stock solution. Second, we calculated the total number of SAMSA molecules bound on the surface of the nanoparticles, based on the fact that the difference in the concentration of SAMSA in the solution before and after the reaction gives the number of SAMSA ligands on the nanoparticles. In this second case, the number of SAMSA molecules per nanoparticle was found to be around 6; part of the reason for this increase is the initial larger concentration of SAMSA (details are in calculation 2). The second method is more accurate for the calculation of number of fluorophores on the surface of the gold.[25]

Under highly acidic conditions, superlattices consisting of Au@MSA/SAMSA could be produced. Figure 2a shows the transmission electron microscopic (TEM) image of a superlattice. Inset I is the fast Fourier transform (FFT) of the image with the diffraction spots labeled, showing an excellent hexagonal arrangement of the nanoparticles. Inset II shows a low magnification image of one edge of the superlattice. Figure 2b is a magnified TEM image of the superlattice, which reveals no further growth of the nanoparticles.

Figure 3I shows field emission scanning electron microscopy (FESEM) images of the triangular superlattice at different tilt angles of a) 0°, b) 20°, c) 40°, and d) 60°. The cross-section thickness of the crystal is found to be ca. 1 μm. Figure 3II shows an energy dispersive analysis of X-rays (EDAX) spectrum collected from the triangle shown in Figure 3I, and the inset shows the corresponding EDAX mapping of the superlattice crystal. All of these establish clearly that the crystals formed are of the monolayer-protected nanoparticles.

The most striking feature of the Au@MSA/SAMSA nanoparticle superlattices concerns their fluorescent nature. Figure 4A shows the fluorescence image of the Au@MSA/SAMSA nanoparticle superlattice. There was no fluorescence for the suspended Au@MSA particles (Fig. 1f). Although no fluorescence image could be obtained for the Au@MSA superlattices within the detection limit of our instrument, a weak Raman image accumulating the intensity in the entire Stokes shift range of 500–3500 cm^{-1} could be collected (Fig. 4B). The optical microscopy images and emission spectra at single spots of the respective superlattices are shown in insets I and II, respectively. The superlattice crystals typically appear as 3D triangles with an edge length of a few micrometers. The emission peak of Au@MSA/SAMSA appears at 675 nm, greatly red-shifted compared to the SAMSA solution sample or an isolated Au@MSA/SAMSA particle (ca. 520 nm). The width of the emission increases from 1731 cm^{-1} in the isolated particles to 3157 cm^{-1} in the superlattice. Both these observations are probably due to the fact that the superlattices have different emission states compared to fluorophores in solution. However, it may be noted that the parent fluorophore, fluorescein isothiocyanate (FITC), shows a red shift of ca. 105 nm in the solid state compared to its emission spectrum in solution,[26] which could be attributed to the intermolecular interaction of the π rings in the solid state. As SAMSA is a FITC-based thiol, a larger red shift is expected here as the fluorophores are expected to have electronic interactions with the molecules and the nanoparticles. The present result clearly indicates that fluorescence superlattices can be built using hydrophilic fluorescent gold nanoparticles.

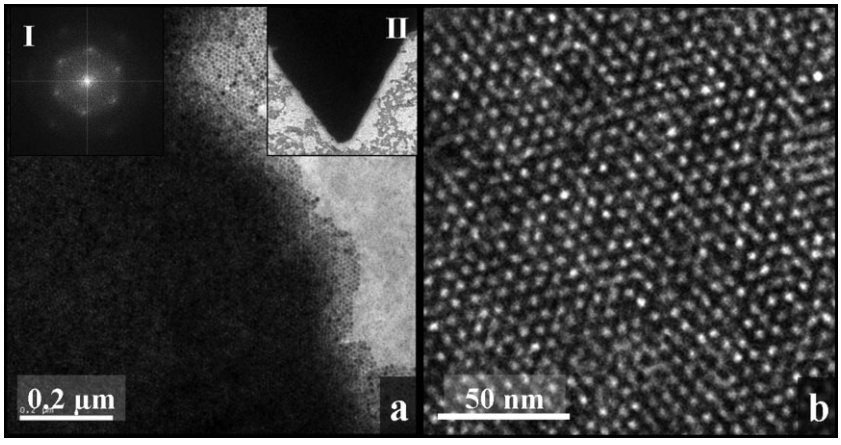

Figure 2. a) TEM image of the Au@MSA/SAMSA superlattice. Inset I: Fast Fourier transform (FFT) of the image. Inset II: Low-magnification image of a superlattice crystal showing the edge that has been magnified in the main part of (a). b) A magnified TEM image of the superlattice showing regularly arranged nanoparticles.

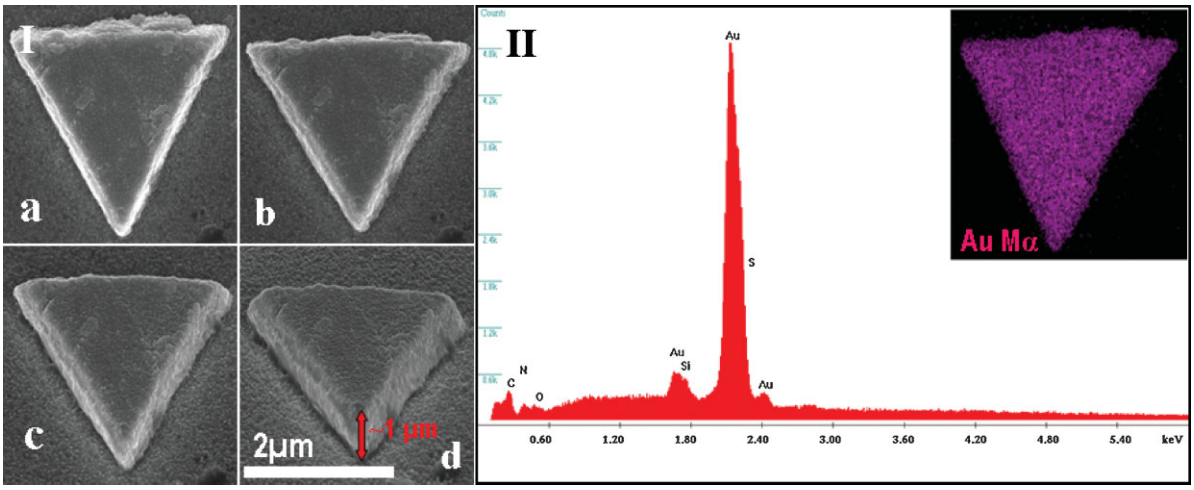

Figure 3. I) FESEM images of superlattice triangles at different tilt angles: a) $\theta = 0°$, b) 20°, c) 40°, and d) 60°. II) EDAX spectrum of the gold superlattice crystal, taken from (Ia). Inset: EDAX mapping of the superlattice triangle using Au M_α.

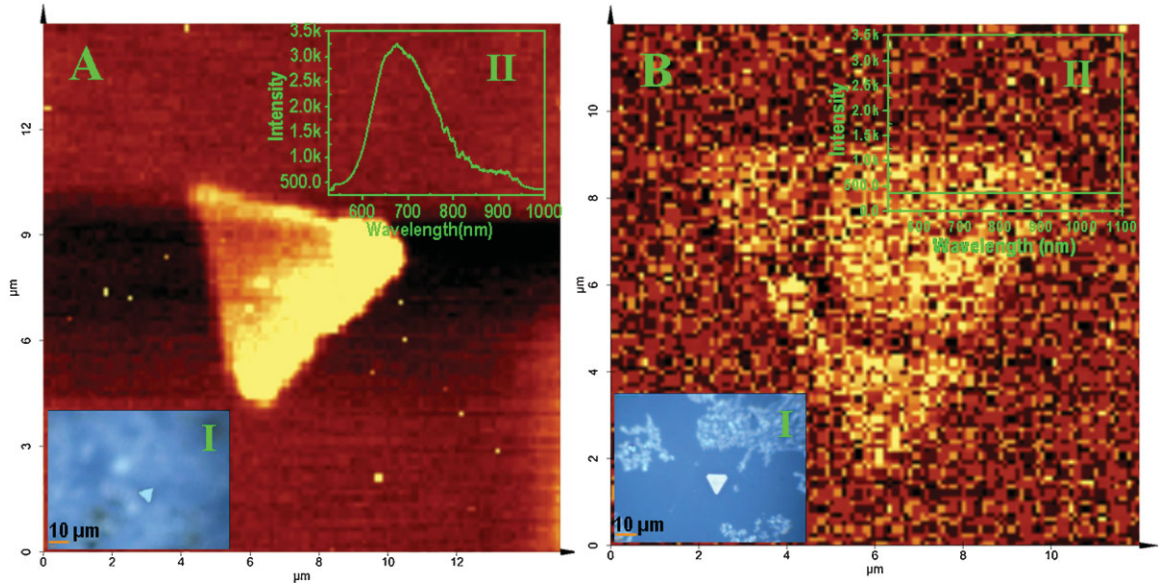

Figure 4. Fluorescence images of superlattice crystals taken with a Raman microscope. Inset I: Optical image of the superlattice crystal. Inset II: Single-spot fluorescence spectrum. Excitation was at 514.5 nm. A) Au@MSA/SAMSA superlattice. B) Au@MSA superlattice.

In conclusion, 3D superlattices of fluorescent gold nanoparticles have been prepared at an air/water interface. Particles of 3.43 nm core diameter exhibit hexagonal assembly extending over several micrometers, and crystals of triangular morphology are observed. The crystals have been imaged using the fluorescence emission of the monolayers protecting the nanoparticles. The superlattices are fluorescent even though SAMSA is close to the metallic core and strong quenching is expected.

Experimental

Materials: All the materials used in this synthesis were purchased from Aldrich, except 5-((2-(and-3)-*S*-(acetylmercapto)succinoyl)amino)-fluorescein (SAMSA), which was purchased from Molecular Probes. The chemicals were used without further purification. SAMSA was activated by dissolving 1 mg SAMSA in 1 mL 0.1 M NaOH and incubating at room temperature for 15 min to remove the acetyl protecting group. Following activation of SAMSA, the solution was neutralized with concentrated HCl and buffered with 0.2 mL of 0.5 M sodium phosphate, pH 7.

Synthesis of Au@MSA: To 50 mL methanolic solution of (0.5 mM) $HAuCl_4 \cdot 3H_2O$, 0.25 mM MSA was added (1:0.5 ratio, total volume of methanol was 50 mL). The mixture was cooled to 0 °C in an ice bath for 30 min. Then an aqueous solution of $NaBH_4$ (0.2 M, 12.5 mL), cooled to 0 °C, was injected rapidly into the above mixture under vigorous stirring. The mixture was allowed to react for another hour. The resulting precipitate was collected and washed repeatedly with methanol through centrifugal precipitation. Finally the Au@MSA precipitate was dried and collected as a dark brown powder [27].

ADVANCED MATERIALS

Anchoring of SAMSA on Au@MSA: Exchange reaction of Au@MSA with SAMSA was carried out in two different concentrations of SAMSA as described below.

Case 1. In a 10 mL solution of Au@MSA (2 mg mL^{-1}), activated SAMSA solution (0.6 mg/5 mL) was dispersed and stirred vigorously for 2 days at room temperature. After the completion of the reaction, the product was precipitated by adding methanol and the precipitate was centrifuged at 10000 rpm. The precipitate was washed repeatedly with ethanol, dispersed in water, and freeze-dried. SAMSA-exchanged Au@MSA is denoted Au@MSA/SAMSA.

Case 2. Here the concentration of SAMSA used for the exchange reaction was 2 mg/5 mL and all the experimental conditions were the same as described above. The ethanol wash was carefully dried and the residue was dissolved in a known amount of water. Absorbance of the above solution was measured and used for the calculation of SAMSA anchoring on the surface of nanoparticles.

Preparation of Gold Nanoparticle Superlattice: The superlattice formation followed an established method [11,14]. The Au@MSA/SAMSA powder (2.0–3.0 mg) was dispersed in distilled water (1.0 mL) and 6 M HCl was added to the nanoparticle solution dropwise to obtain a pH 0.7–0.9. The dispersion was left undisturbed for a week in the dark at a temperature below 25 °C. After 7 days of storage, crystallization took place at the air/water interface. A film with a mirror-like appearance was seen, indicating the formation of gold nanoparticle superlattices. But the quality of the superlattice crystal was poor at the initial stage of film formation; it takes a minimum 2–3 weeks for the formation of quality crystals. After the formation of superlattices, the film was transferred to a thin glass plate for Raman and fluorescence measurements. FESEM measurements were done by transferring the film onto the surface of a polished silicon wafer.

Raman and Fluorescence Observations: The Raman and fluorescence spectra were collected with a 514.5 nm Ar ion laser from a spot size <1 μm. The laser had a maximum power of 40 mW. The back-scattered light was collected by a 100× objective lens and sent to the spectrometer through a multimode fiber. A super-notch filter placed in the path of the signal effectively cuts off the excitation radiation. The signal was then dispersed using a 150 grooves/mm grating and the dispersed light was collected by a Peltier-cooled charge coupled device (CCD). Single-spot spectra were also acquired using the same grating but with longer integration times. For improved resolution and to ascertain the peak positions, a grating with 1800 grooves/mm was also used while acquiring single-spot spectra. The effective scan range of the spectrometer was 0–9000 cm^{-1} (amounts to a wavelength maximum of 958.2 nm for 514.5 nm excitation), with detection efficiency falling above 750 nm. For spectral imaging, the desired area was partitioned into 10000 squares (an imaginary 100 × 100 matrix drawn over it), with each square representing a sampling point and consequently a pixel for the image. Typical signal acquisition time at each pixel of the image was 0.1 s. The intensities of the desired portion of the spectra collected over all the pixels were compared by ScanCTRL Spectroscopy Plus Version 1.32 software, to construct a color-coded image. Thus, for the images presented in this Communication, regions coded yellow represent the pixels where the signal (used for mapping) is maximum, the minimum being represented by red/black colors.

UV-vis absorption spectra were recorded using a PerkinElmer Lambda 5 spectrometer. Emission spectra were measured using an F-4500 Hitachi spectrofluorimeter. The bandpass for excitation and emission was set as 5 nm.

HRTEM and Spectroscopic Measurements: To study the structure of the superlattice, high-resolution transmission electron microscopy (HRTEM) was carried out with a JEOL 3010 UHR instrument. The sample was prepared by lifting the superlattice film onto carbon-coated copper grids and drying in ambient atmosphere. The sample was observed at 200 keV to reduce electron-beam-induced damage.

FESEM Measurements: FESEM measurements were done using a FEI NOVA NANO SEM 600.

Calculation of the number of SAMSA molecules per nanoparticle:

Calculation 1 for Case 1: Using the emission intensity.

Total number of gold particles synthesized

$$N = \frac{m_g}{(4/3)\pi r^3 \rho_g} \tag{1}$$

where m_g is the total mass of gold, the radius of the nanoparticle $r = 1.715$ nm (from TEM), and the density of gold $\rho_g = 19.3$ g/cm^3. Thus for $m_g = 9.85 \times 10^{-2}$ g

$$N = \frac{9.85 \times 10^{-2}}{4.08 \times 10^{-19}} = 2.41 \times 10^{17} \tag{2}$$

Intensity ratio from the emission spectra of Au@MSA/SAMSA and SAMSA = 0.163.

Total number of SAMSA molecules in the solution (10^{-6} M, 5 mL) is

$$\begin{aligned} z &= 10^{-6} \times (6.023 \times 10^{23}) \times (5 \times 10^{-3}) \\ &= 3.012 \times 10^{15} \end{aligned} \tag{3}$$

Total number of SAMSA molecules in Au@MSA/SAMSA is $0.163z = 4.909 \times 10^{14}$.

Number of Au particles in the cuvette (for 0.2 mg gold) is

$$y = \frac{0.2 \times 10^{-3}}{(4/3)\pi r^3 \rho_g} = 4.902 \times 10^{14} \tag{4}$$

Number of SAMSA molecules in 1 gold nanoparticle = $(4.909 \times 10^{14})/(4.902 \times 10^{14}) = 1.001$.

Calculation 2 for Case 2: Using the molar extinction coefficient of SAMSA.

The calculation involves three steps: 1) Calculation of the number of gold nanoparticles in the stock solution. 2) Calculation of the total number of SAMSA ligands on the nanoparticles. 3) Calculation of the number of SAMSA ligands per nanoparticle.

1) Calculation of the number of nanoparticles in the stock solution.

Average number of gold atoms per nanoparticle

$$N_{av} = \frac{\pi D^3}{6} \rho \left(\frac{1}{M}\right) \tag{5}$$

where D is the diameter of the nanoparticles and M is the atomic weight of gold.

Molar concentration of nanoparticle solution

$$C = N_{\text{total}}/N_{\text{av}} V N_A$$

where $N_{\text{total}} = 1.5 \times 10^{20}$ atoms, V is the volume, and N_A is Avogadro's number.

Hence molar concentration $C = 19.97$ nM.

Number of moles $m = CV/1000 = 0.009985 \times 10^{-10}$.

Number of gold nanoparticles in stock solution is $mN_A = 6.013 \times 10^{11}$.

2) Calculation of number of SAMSA ligands on the nanoparticles.

Concentration of SAMSA used for exchange reaction $C_1 = 3.17 \times 10^{-6}$ M.

Extinction coefficient $\varepsilon_{\text{SAMSA}} = 5.84 \times 10^4$ M^{-1} cm^{-1}(calculated from UV/vis data).

After exchange reaction, the product was precipitated and the supernatant was carefully concentrated to a known volume. From the standard volume, a known amount was taken out for the absorbance measurements and the concentration of unbound SAMSA molecules was calculated.

Concentration of unbound SAMSA molecules $C_2 = 2.75 \times 10^{-6}$ M.

Therefore, the concentration of SAMSA ligands bound on nanoparticles is $C_1 - C_2 = 0.42 \times 10^{-6}$ M.

Number of moles is $0.00000630 \times 10^{-6}$.

Number of SAMSA ligands bound on nanoparticles is 37.9×10^{11}.

3) Calculation of number of SAMSA ligands per nanoparticle.

Number of SAMSA ligands per nanoparticle

$$N_{\mathrm{SAMSA/np}} = \frac{\text{number of bound SAMSA ligands}}{\text{number of nanoparticles in the stock}} = \frac{37.9 \times 10^{11}}{6.013 \times 10^{11}} \approx 6 \text{ SAMSA molecules per nanoparticle}$$

Received: March 5, 2008
Revised: March 25, 2008
Published online: July 17, 2008

[1] M. C. Daniel, D. Astruc, *Chem. Rev.* **2004**, *104*, 293.
[2] R. L. Whetten, M. N. Shafigullin, J. T. Koury, T. G. Schaaff, I. Vezmar, M. M. Alvarez, A. Wilkinson, *Acc. Chem. Res.* **1999**, *32*, 397.
[3] M. Brust, M. Walker, D. Bethell, D. J. Schiffrin, R. Whyman, *J. Chem. Soc, Chem. Commun.* **1994**, 801.
[4] A. C. Templeton, W. P. Wuelfing, R. W. Murray, *Acc. Chem. Res.* **2000**, *33*, 27.
[5] S. A. Harfenist, Z. L. Wang, R. L. Whetten, I. Vezmar, M. M. Alvarez, *Adv. Mater.* **1997**, *9*, 817.
[6] J. R. Heath, C. M. Knobler, D. V. Leff, *J. Phys. Chem. B* **1997**, *101*, 189.
[7] M. P. Pileni, *J. Phys. Chem. B* **2001**, *105*, 3358.
[8] S. Stoeva, K. J. Klabunde, C. M. Sorensen, I. Dragieva, *J. Am. Chem. Soc.* **2002**, *124*, 2305.
[9] I. Lisiecki, *J. Phys. Chem. B* **2005**, *109*, 12231.
[10] E. V. Shevchenko, D. V. Talapin, N. A. Kotov, S. O'Brien, C. B. Murray, *Nature* **2006**, *439*, 55.
[11] K. Kimura, S. Sato, H. Yao, *Chem. Lett.* **2001**, *372*.
[12] S. Sato, H. Yao, K. Kimura, *Physica E* **2003**, *17*, 521.
[13] H. Yao, H. Kojima, S. Sato, K. Kimura, *Langmuir* **2004**, *20*, 10317.
[14] S. H. Wang, S. Sato, K. Kimura, *Chem. Mater.* **2003**, *15*, 2445.
[15] S. H. Wang, H. Yao, S. Sato, K. Kimura, *J. Am. Chem. Soc.* **2004**, *126*, 7438.
[16] Y. Yang, S. Liu, K. Kimura, *Angew. Chem, Int. Ed.* **2006**, *45*, 5662.
[17] S. Chen, R. S. Ingram, M. J. Hostetler, J. J. Pietron, R. W. Murray, T. G. Schaaff, J. T. Khoury, M. M. Alvarez, R. L. Whetten, *Science* **1998**, *280*, 2098.
[18] J. J. Hickman, D. Ofer, P. E. Laibinis, G. M. Whitesides, M. S. Wrighton, *Science* **1991**, *252*, 688.
[19] R. Elghanian, J. J. Storhoff, R. C. Mucic, R. L. Letsinger, C. A. Mirkin, *Science* **1997**, *277*, 1078.
[20] A. Aguila, R. W. Murray, *Langmuir* **2000**, *16*, 5949.
[21] T. Gu, J. K. Whitesell, M. A. Fox, *Chem. Mater.* **2003**, *15*, 1358.
[22] A. C. Templeton, D. E. Cliffel, R. W. Murray, *J. Am. Chem. Soc.* **1999**, *121*, 7081.
[23] E. Dulkeith, A. C. Morteani, T. Niedereichholz, T. A. Klar, J. Feldmann, S. A. Levi, F. C. J. M. van Veggel, D. N. Reinhoudt, M. Motter, D. I. Gittens, *Phys. Rev. Lett.* **2002**, *89*, 203002.
[24] P. P. H. Cheng, D. Silvester, G. Wang, G. Kalyuzhny, A. Douglas, R. W. Murray, *J. Phys. Chem. B* **2006**, *110*, 4637.
[25] P. Pramod, P. K. Sudeep, K. G. Thomas, P. V. Kamat, *J. Phys. Chem. B* **2006**, *110*, 20737.
[26] P.-S. G. Kim, N. O. Petersen, T. K. Sham, Y. F. Hu, *Chem. Phys. Lett.* **2004**, *392*, 44.
[27] S. Chen, K. Kimura, *Langmuir* **1999**, *15*, 1075.